Simulation of the Power Transmitted by Various Waveguides: Version 3

M. Leber

Department of Physics, University of California, Santa Barbara, CA

(Dated: June 2, 2011)

In this document, we outline the simulation of power transmitted by various waveguides. Higher harmonics, magnetic field variation, the doppler shift, reflections, and losses are investigated.

CONTENTS

I. SIMULATION PROCESS

Simulating the transmission-line prototype is a three-step process; first the electron is tracked in the magnetic field and the position versus time is recorded; second, the spectral components of the radiated power are calculated; finally, the power spectrum is filtered and mixed down to match the expected signal. The run parameters for all codes are set in a central file with a ".ini" extension.

A. Magnetic Field Calculation and Electron Tracking: Adipark

The electron is tracked using Thomas Thuemmler's adipark. This code optionally utilizes the Legendre polynomial expansion of Ferenc Glueck's magfield2 to calculate the magnetic field. The source points are read in at run time, so they must first be calculated from the coil geometry by magfield2. Adipark assumes the motion is adiabatic; it uses a second-order Runge-Kutta midpoint method to calculate the guiding center motion along a field line including gradient and curvature drifts. Radiative energy loss is calculated in free space, but may be larger near transmission lines, especially when reflections are included. Each step is written to a text file. Adipark's time steps are variable length and depend on the change in magnetic field.

B. Radiation Calculation: Adi2fft

The radiation collected by the transmission line is calculated using adi2fft, originally written by Ben Monreal. Adi2fft reads in the adipark steps and interpolates between points to get evenly spaced time steps at the readout end of the antenna. The user chooses between various transmission lines: parallel wires, parallel strips, or a coaxial cable. The amplitude of the dominant waveguide mode excited by the electron, $A * c(t)$, is calculated from the retarded time, position, phase, and velocity of the electron and $A * c(t)$ is converted to a voltage $v(t)$. Reflections from the other end of the antenna and noise can also be included. The time-series of voltage or field amplitude at the readout end is Fourier transformed to calculate the spectral components of the transmitted power. This is a discrete Fourier transform of $A * c(t)$, so there are multiple definitions of the power spectrum computed from $A * C(f)$, as discussed below. In all cases we calculate a one-sided power spectrum; the

negative frequencies are added into the positive frequencies. The results are written to a ROOT file.

C. Filtering and Mixing: Adifilter

Filtering and mixing are easily accomplished in frequency space. New code called adifilter reads in the spectral components of the power, filters to reduce the bandwidth and mixes with a local oscillator to reduce the frequency. The result is inverse Fourier transformed to create a time series the same length, but much lower sampling frequency, similar to the data format. Noise can also be added at this stage. The results are written to a ROOT file.

Another optional analysis step is to Fourier transform the filtered and down-mixed time series to produce a two dimensional spectrogram or "spectral waterfall" plot, the power versus frequency and time. This code is called adiplot.

II. SIMULATION DETAILS AND BENCHMARKS

Here we discuss the details of the simulation.

A. Energy Loss

To keep the electron tracking separate from the radiation near transmission lines, adipark calculates the energy lost by electrons into free space, although the total energy loss near a transmission line is slightly larger without reflections, and four times larger for during the constructive interference (or stimulated emission) of reflections.

In adipark, electrons are losing energy as they radiate, at a rate of 1.13 fW for 17.8 keV electrons in free space. The shift in frequency due to energy loss is equal to the frequency bin width for tracking times of:

$$T = \sqrt{\frac{E}{pf}} = 50\mu\text{s} \tag{1}$$

where E is the total electron energy (528.8 keV), p is the power lost to cyclotron radiation, and f is the frequency. To reach a higher signal to noise, we may track for longer than 50 μs, but may need to account for the energy loss.

B. Power Spectra and Windowing

There are many possible definitions of discrete power spectra. In this section, we define multiple power spectra and calculate and compare the time-averaged power from these power spectra.

In adi2fft, we use three methods to calculate the time-average power from the discretely sampled signal. First, in the time domain, we can calculate the instantaneous power at discrete time points, $P(t)$, integrate this sampled power over the time duration, and normalize by the time duration. Second, we can use FFTW to discretely Fourier transform the signal to calculate a digitized version of the power-spectral density $P(f)$, which must be integrated over the relevant frequency range to get the time-averaged power. Third, instead of creating an approximate continuous power spectrum, we create the discrete-valued power at the given frequency bin. This does not require an integral.

A simple way to compare these methods is to track an electron in a constant 1 T field and use $A * c(t) = \cos\phi(t)$. The time-average of $\cos^2\omega t$ is 1/2, so with our definitions this example should give a time-averaged power of $\bar{P} = 1/2Z = 1.3 * 10^{-22}$fW.

To calculate the time-averaged power in the time domain (the first method), we need the instantaneous power, $P(t) = [A * c(t)]^2/Z = \cos^2\phi(t)/Z$. This is fit to $\cos^2 2\pi ft$, integrated over the fit range T, and normalized by T. The fit is shown in Fig. 1a. The power calculated this way is $1.4 * 10^{-22}$ fW, consistent with the expectation.

In the frequency domain (the second method) an electron moving in a constant magnetic field would create a delta function in $P(f)$ centered at $f_0 = 27.049$ GHz if the signal has infinite duration. But the signal is finite in time, which modifies the shape of the peak. Since the signal turns on and off sharply, the window function is rectangular, and $P(f)$ has the shape [4]:

$$\left[\frac{\sin(\pi(f-f_0)T)}{\sin(\pi(f-f_0)T/N)}\right]^2 \approx \left[\frac{\sin(\pi(f-f_0)T)}{\pi(f-f_0)T}\right]^2 \text{(large sampling freq.)} \tag{2}$$

where T is the electron's total time-of-flight. Another window, for example the Hann window, may prevent spectral leakage.

This discussion assumes the frequency bin width is large compared to the frequency shift due to radiative energy loss. Without correction for energy loss, the peak in the power spectrum will shift.

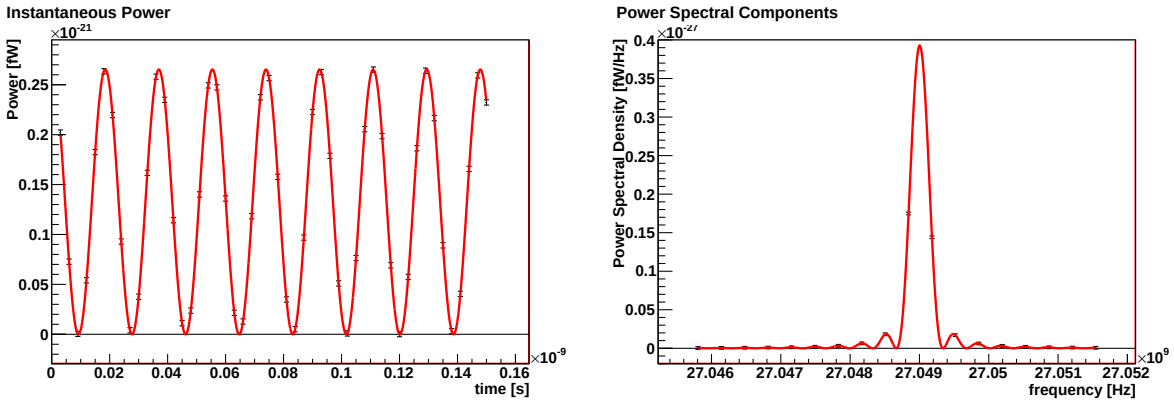

FIG. 1. Time-averaged power can be calculated from approximate continuous distributions $P(t)$ (left) or $P(f)$ (right) by fitting and integrating. On the left, this simplest case shows the power calculated from $Ac(t) = \cos\phi(t)$, and the instantaneous power $P(t)$ is fit to $\cos^2 2\pi ft$. On the right, the approximate power spectral density is fit to $\sin^2 x/x^2$, where $x = \pi(f - f_0)/T$, since the signal is finite and windowed with a rectangular function.

In addition, the signal and Fourier transform are discrete, so $P(f)$ is not continuous. In the time domain, the discrete signal is sampled from the continuous signal:

$$c_k = c(t_k) \tag{3}$$

Therefore the discrete instantaneous power is the same as the continuous function evaluated at the time-bin center:

$$P_k = P(t_k) = \frac{1}{Z}|A * c_k|^2 = \frac{1}{Z}|A * c(t_k)|^2 \tag{4}$$

The discrete Fourier transform defined by FFTW is:

$$C_n = \sum_{k=0}^{N-1} c_k e^{2\pi ikn/N} \tag{5}$$

Therefore, in frequency space, the discrete values are multiplied by the time step Δ_t:

$$C(f_n) \simeq \Delta_t * C_n \tag{6}$$

$$P(f_n) = \frac{1}{ZT_{max}}|A * C(f_n)|^2 \simeq \frac{1}{ZT_{max}}|A * \Delta_t * C_n|^2$$

Fig. 1 shows this approximate power spectral density and the fit to $\sin^2 x/x^2$ function. Once the function is integrated, the time-averaged power is $2.1 * 10^{-22}$ fW, more than expected.

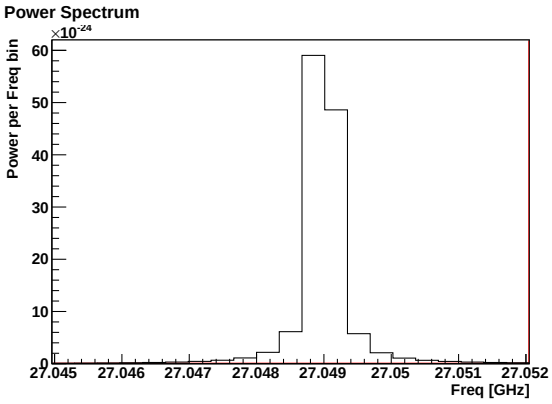

FIG. 2. The time-averaged power is defined at each frequency bin, but the power in the peak is shared between two bins.

TABLE I. For a discrete time series with time step Δ_t and integration time T_{max}, the power spectrum can be defined multiple ways. The Fourier transform bin width Δf is $1/T_{max}$. For all definitions, the signal to noise increases linearly with T_{max}.

Power Spectrum	**Definition**	**Expected Signal**	**Mean Noise (λ)**
Power Spectral Density	$P(f_n) = \frac{1}{ZT_{max}}\|A * \Delta_t * C_n\|^2$	$\bar{P}/\Delta f$	kT
Energy Spectral Density	$E(f_n) = \frac{1}{Z}\|A * \Delta_t * C_n\|^2$	$\bar{P}T_{max}/\Delta f$	$kT * T_{max}$
Power per bin	$P_n = \frac{\Delta f}{ZT_{max}}\|A * \Delta_t * C_n\|^2$	$\bar{P}$	kT/T_{max}
Energy per bin	$E_n = \frac{\Delta f}{Z}\|A * \Delta_t * C_n\|^2$	$\bar{P}T_{max}$	kT

Finally, in the third method, we calculate the power per frequency bin, or multiple by the frequency bin width Δf so that:

$$P_n = \frac{\Delta f}{ZT_{max}}|A * \Delta_t * C_n|^2 \tag{7}$$

This is shown in Fig. 2. The time-averaged power is split between two bins; added together the total is $1.1 * 10^{-22}$, slightly less than expected. This method is the easiest and most consistent, but depending on where the central frequency falls within bins, power can be split between two bins.

Table I shows the multiple definitions of the power spectra.

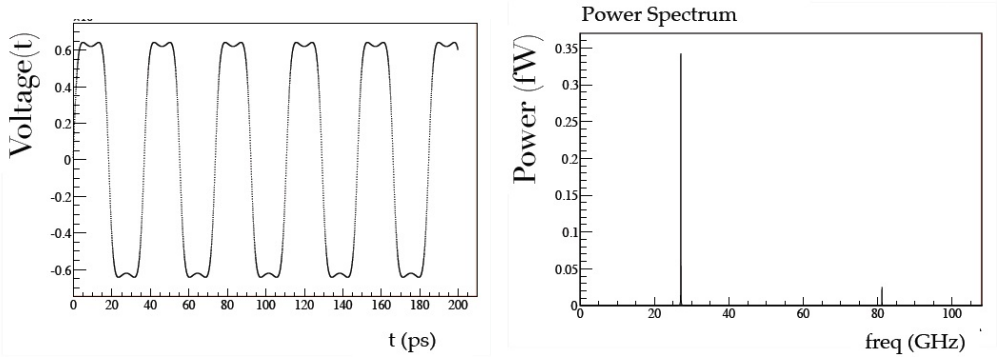

FIG. 3. Power transmitted by a parallel-wire with an electron circling centrally between the wires. In a constant 1 T field, the central frequency is 27 GHz, and the third harmonic is 81 GHz. The higher harmonics are excited because the electric field changes over an orbit.

C. Electric Fields

The power collected by a transmission line depends on the modes of the line. All modes or electric fields used in adi2fft are analytic. Therefore, any mis-alignments and the effects of external components (like the trapping coil) are not included. These fields are listed in [3].

1. Higher Harmonics

Higher harmonics are excited because the electric field changes over the electron's orbit. The field changes the most when the electron is close to a wire. To observe this effect, we track an electron centered between two wires in a constant magnetic field and include the gyroradius in the electron's motion. Fig. 3 shows the time-domain signal and the resulting power spectrum. The first harmonic is 27 GHz (for 1 T field) and the third harmonic is at 81 GHz.

D. Interpolation and Doppler Shift

The analytic doppler shift discussed in [3] cannot be used in the simulation because it is not a pure Fourier transform; the time-domain function $A * c(t)$ in Eq. 9 contains the variable ω within the wavenumber k. An easier method is to calculate the field amplitude

excited at the electron, or some fixed distance from the electron, then calculate the time delay for the signal to reach the antenna or end of the transmission line. As the electron moves, the distance to the antenna or transmission line end changes, introducing a doppler shift.

In adi2fft, evenly spaced time steps at the read-out end of the transmission line are necessary for a discrete Fourier transform. The exact position of the read-out end does not matter, a shift in this position just introduces a constant time delay. We use the position of the connection to the balun as the end of the transmission line, and from here on refer to this as the antenna.

A wave emitted at the retarded time t_r at position $x(t_r)$ arrives at the antenna position x_{ant} at the antenna time t_a:

$$t_a = t_r + x_{\text{ant}}/c - x(t_r)/c \tag{8}$$

Since the electron is moving, the distance to the antenna changes and depends on the retarded time t_r. We choose evenly spaced antenna times, and calculate the retarded time as:

$$t_{r,n} = t_{a,n} - x_{\text{ant}}/c + x(t_{r,n-1})/c \tag{9}$$

As an approximation, we use the electron position at the previous time step.Then we read in the adipark track steps and interpolate between values of velocity and position. Finally, we calculate the field amplitude at the retarded time as:

$$A * c(t_a) = -\frac{qZ}{2}\left[\mathbf{v}_t(t_r) \cdot \mathbf{E}_t(r_0(t_r)) \pm v_z(t_r) \cdot E_z(r_0(t_r))\right] \tag{10}$$

To observe the effect of the doppler shift, we track an electron through a constant magnetic field and calculated the power from $A * c(t_a) = \cos\phi(t_r)$. Three electrons are tracked with pitch angles of 89.9°, 90.0°, and 90.1°. The power spectrum is shown in Fig. 4. The shift in frequency, 12 MHz, is correct for this electron trajectory. The total time-average power radiated is roughly the same when the doppler shift is included and neglected.

E. Magnetic Fields

Adipark has three ways to calculate a magnetic field: use a constant field, use a parabolic field, or calcualte the field using magfield2 of Ferenc Glueck. We've used all three methods for testing.

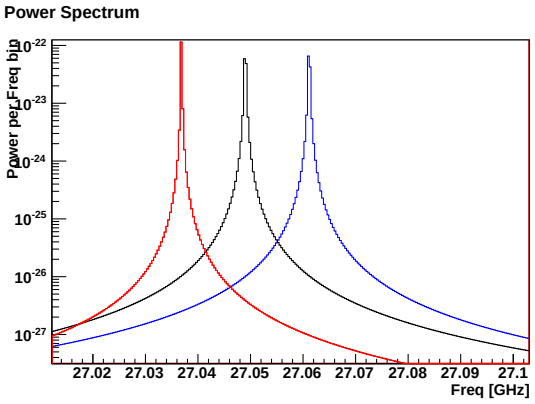

FIG. 4. Power transmitted down a parallel wire transmission line for an electron in a constant magnetic field. In red, a pitch of 90.1°, in black, a pitch angle of 90.0°, and in blue, 89.9°. The doppler shift causes a shifted peak.

1. *Pure Parabolic Field*

The central frequency is determined by average magnetic field, which changes for different pitch angles and radial position within the magnet.

$$\bar{f_0} = f_0 \left(1 + \frac{\cos^2\theta}{2\sin^2\theta}\right) \tag{11}$$

Splitting to first sideband is:

$$\Delta f = \frac{\beta c \sin\theta}{2\pi L} \tag{12}$$

2. *Magnetron Drift*

If the electron is not orbiting around the magnetic axis of symmetry, the gradient and curvature drifts cause the guiding center to rotate about the magnetic axis. Both drifts depend on the the gradient and curvature of the field at the guiding center, the charge of the particle, and the pitch angle of the particle. Neither depends on the direction of the guiding center velocity, so the drift direction is the same regardless of the direction of the electron in the trap. The drift velocity of the guiding center is:

$$u_\perp = \frac{1}{\omega R}\left(\frac{v_\perp^2}{2} + u_{||}^2\right)\left(\frac{\mathbf{R}\times\mathbf{B}}{RB}\right) = \left(\frac{\mu}{q} + \frac{m u_{||}^2}{Bq}\right)\left(\frac{\mathbf{B}\times\boldsymbol{\nabla}_\perp B}{B^2}\right) \tag{13}$$

where $v_\perp$ is gyration velocity. The magnetron frequency is 0.5 MHz for a 89° electron in the magnetic trap. The magnetic gradient drift will move electrons toward and away from the wires, causing an amplitude modulation at 0.5MHz or more. The gradient force is clockwise in the y-z plane.

F. Reflections

If the transmission line is not terminated, the backward wave will reflect. The amplitude of a reflected wave depends on how the transmission line is terminated and the reflection coefficient:

$$\Gamma_L = V_0/V_{\rm ref} = \frac{\bar{Z}_L - 1}{\bar{Z}_L + 1} \tag{14}$$

The time it takes for a reflected wave to reach the antenna end depends on the position of reflection $x_{\rm ref}$ and the position of the antenna $x_{\rm ant}$. The position of reflection is the unterminated end of the transmission line with respect to the center of the trapping coil. As discussed in Section II D, the antenna position is designated as the connection to the balun, but has no physical significance except an overall time shift. The time the reflected wave reaches the antenna is:

$$t_a = t_r + (x_{\rm ant} + 2x_{\rm ref})/c - x(t_r)/c \tag{15}$$

We must interpolate between points to get evenly spaced antenna times, then evaluate the electron parameters at this retarded time:

$$t_{r,n} = t_{a,n} - (x_{\rm ant} + 2x_{\rm ref})/c + x(t_{r,n-1})/c \tag{16}$$

As an approximation, we use the electron position at the previous time step.

The reflected wave emitted at t_r will add to the forward wave emitted at a later time t_f. The time difference between interfering waves is:

$$\Delta t = (2x_{\rm ref} + x(t_r) + x(t_f))/c \tag{17}$$

This time difference causes a phase difference of:

$$\phi = \omega\Delta t = 2\pi(2x_{\rm ref} + x(t_r) + x(t_f))/\lambda \tag{18}$$

When this phase difference is a integer multiple of 2π, the waves constructively interfere. In the UW prototype, the wavelength λ is 1.1 cm, $x_{\rm ref}$ is 3.3 cm, and the maximum displacement for a 89° electron is about 2 mm. If the reflected wave and the forward wave are emitted from the center of the trap ($x(t_r) = x(t_f) = 0$), constructive interference occurs. If the reflected wave and forward wave are both emitted at the edges of the trap, the least constructive interference occurs, but is still greater than no reflections for pitch angles greater than 89°.

G. Losses

Power can be lost along the transmission line due to resistance of the copper and conductance of the dielectric support. The lines used in the UW prototype are low-loss lines, so the voltage and power will be attenuated by:

$$V(z_{ant}) = V_0 e^{-\alpha z_{ant}} \tag{19}$$

$$P = V_0^2/Z_c e^{-2\alpha z_{ant}} \tag{20}$$

where z_{ant} is the distance the radiation must travel to reach the readout end of the line (the balun) and $\alpha = (R/Z_c + GZ_c)/2$ is the attenuation constant.

The resistance per unit length R is different for each transmission line and is defined in [3]. It depends on the skin depth, which is weakly frequency dependent. The attenuation coefficient due to resistance is largest for the parallel wires, at 0.0011/cm. For the parallel strips, it is 0.0002/cm.

The UW prototype is supported by a Rogers Duroid 5870 dielectric. If the transmission line was completely surrounded by dielectric, the shunt conductance would $G = \omega\epsilon''/\epsilon' C = \omega \tan\delta C$. For this dielectric, $\tan\delta = 0.0012$. We use the attenuation coefficient assuming the lines are surrounded by dielectric. The coefficient for partial dielectric coverage is likely to be smaller. It is the same for all lines, 0.0034/cm.

Reflected signal travel farthest on the transmission line, a maximum of about 10 cm. In this case, the signal is attenuated by less than 5%.

For the UW prototype at 1 T field, the attenuation coefficient will change little over the frequency range, since $\alpha = \alpha_R\sqrt{\omega/27\text{GHz}} + \alpha_G\omega/27\text{GHz}$.

H. Noise

For now, we assume the noise is thermal, johnson, or white noise and is independent of frequency. In the simulations, the noise temperature is the temperature of the cavity, 35 K, plus the noise temperature of the amplifier, 25 K. The noise level is the same regardless of how the antenna is terminated, but terminating with a resistor may increase the noise.

1. Time Domain Noise

In the time domain, thermal noise introduces a random gaussian voltage fluctuation with mean of zero and variance $\sigma^2 = kTf_{max}Z_c$ (units volts), where f_{max} is the bandwidth or the Nyquist frequency $1/2\Delta_t$. The PDF for a voltage v is:

$$PDF(v) = \frac{1}{\sqrt{2\pi\ \sigma^2}} e^{-v^2/2\sigma^2} \tag{21}$$

The PDF for the electric field amplitude is also a normal distribution with a variance of $\sigma^2 = kTf_{max}Z_0$, where the characteristic line impedance is replaced with the wave impedance.

The instantaneous power (in the time domain) is proportional to the square of the voltage ($p_t = v^2/Z_c$), so the PDF is:

$$PDF(p_t) = \sqrt{\frac{Z_c}{2\pi\sigma^2 p_t}} e^{-p_t Z_c/2\sigma^2} \tag{22}$$

The mean of this distribution is σ^2/Z_c and the variance is $2\sigma^4/Z_c^2$.

2. Frequency Domain Noise

In frequency domain, the thermal noise power distribution is chi-square distribution with two degrees of freedom, or an exponential. The PDF for a continuous power $P(f)$ (as defined in Eq. 6) is:

$$PDF(P(f)) = \frac{1}{\lambda} e^{-P(f)/\lambda} \tag{23}$$

where $\lambda = kT$. The mean of this distribution is λ and the variance is λ^2. Because the variance is so large, we need a total power of 4.6 times the noise to have 99% confidence that a fluctuation in a single bin is not noise.

All of the various definitions of the power spectrum exhibit an exponential distribution for the thermal noise power, but have different definitions of the mean λ, which is listed in Table I. The signal to noise ratio is also the same for every definition of the power spectra, as you can see by dividing the expected signal by the mean noise for every row of Table I. Eq. 23 is the noise PDF for the approximate continuous power spectral density, with $\lambda = kT$; in this case the noise level is constant with integration time, but the width of the signal peak decreases with larger integration times. Alternatively, the noise PDF for a power P_n in frequency bin n (defined in Eq. 7) has mean noise $\lambda = kT/T_{max}$, so the noise decreases with integration time but the signal time-averaged power remains the same. With an integration time of 50 μs, the mean noise λ per frequency bin is $1.6 * 10^{-2}$ fW. Regardless of how you calculate the power spectrum, the signal to noise ratio in the frequency domain increases linearly with integration time.

3. Filtering and Averaging Spectra

For the simulation, noise is added to the signal in the time domain. Random voltages are chosen from the PDF for voltage, which depends on the bandwidth or sampling frequency. When noise is added in adi2fft, the bandwidth is the Nyquist frequency because there is no filtering. If the noise is added in adifilter, the bandwidth only the width of the filter, which is half the sampling frequency of the oscilloscope. Either way, the SNR in the frequency domain is unaffected. Filtering out frequencies reduces the bandwidth and noise in the time domain. Only longer integration times reduce the noise in the frequency domain.

Instead of Fourier transforming a long time series, multiple power spectra can be averaged together to improve the SNR and correct for energy loss. When N independent variables from exponential distributions are summed together (for example, averaging power spectra), the resultant PDF is an Erlang distribution. Defining the averaged power as $\bar{P} = \Sigma_{i=1}^{N} P_i/N$, the distribution is:

$$PDF(\bar{P}) = \frac{N^N \bar{P}^{N-1}}{\lambda^N (N-1)!} e^{-N\bar{P}/\lambda} \tag{24}$$

The mean noise still λ, but the noise variance is now λ^2/N. The signal power to noise power does not improve with more averaging, but the mean to standard deviation ratio improves as $\sqrt{N}$.

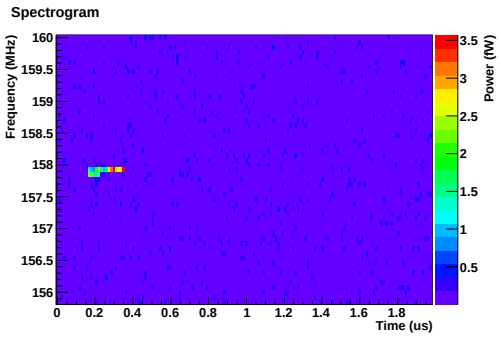

FIG. 5. Power transmitted by a parallel-wire for an electron trapped in the UW prototype, including doppler shift.

III. RESULTS

There are two convincing signatures of a trapped electron that we could hope to observe; first, a high power peak shifting in frequency with the rate expected from energy loss; second, high power peaks split in frequency expected of the central to side band splitting. The first should be relatively easy to observe if electrons with pitch angles greater than 89° can be trapped for 200 μs or more without scattering. A typical spectrogram is shown in Fig. 5. The second will be much harder. We discuss the possibility of observing the sidebands for terminated and open parallel wires.

A. Terminated Wires (no reflections)

Energy loss near the terminated wire transmission line is the same as in free space, so the energy resolution is equal to the energy shift for observation times of $50\mu s$. The mean noise in this time is 0.016 fW. Fig. 6 shows the expected power spectrum without noise for various pitch angles. The first sidebands for 89° electrons may be visible above the 0.016 fW noise.

If the electron can be observed for longer periods without scattering, for $200\mu s$ for example, the power spectra must be averaged to correct for energy loss. Fig. 7 shows the shifting frequency peak, and four power spectra averaged together.

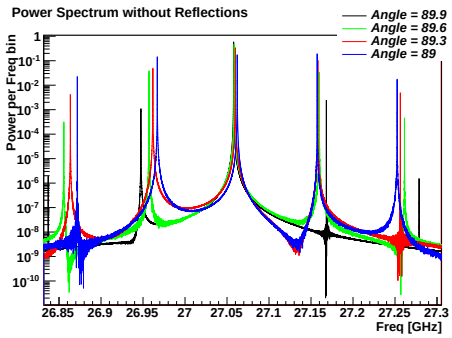

FIG. 6. Power transmitted by a parallel-wire for an electron trapped in the UW prototype with terminated parallel wire transmission line, including doppler shift. No noise is added to this spectra. The ratio of power in the central peak to the sidebands changes with pitch angle.

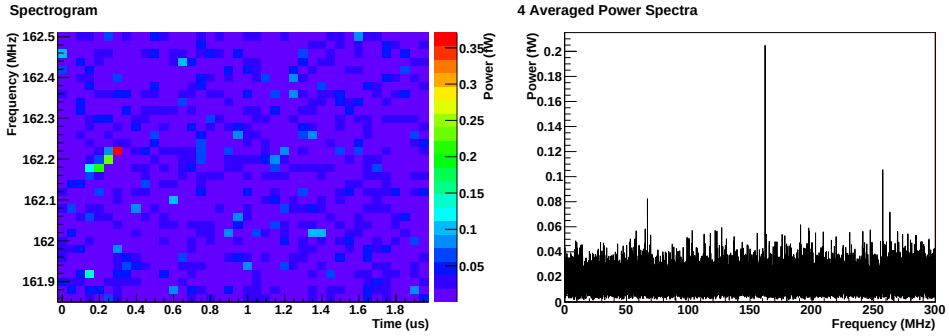

FIG. 7. Spectrograph from a terminated parallel wire transmission line, including doppler shift and noise. On the right, the four high-power bins are averaged together and the sidebands are visible above the noise.

B. Open Wires (with reflections)

The power collected by an open transmission line is four times higher due to constructive interference. The reflected wave must cause stimulated emission at the electron, so four times the power is emitted. In this case, energy resolution is equal to energy shift due to radiation for observation times of 13 μs. The noise per bin is 0.06 fW. Fig 8 shows the expected power spectra without noise for various pitch angles. The second sideband has higher power than the first.

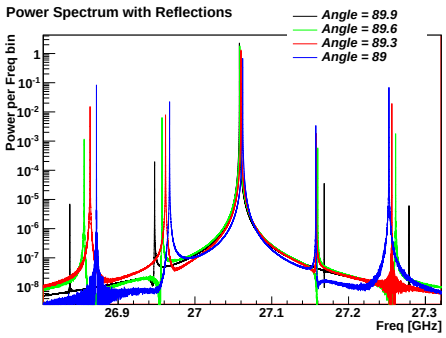

FIG. 8. Power transmitted by a parallel-wire for an electron trapped in the UW prototype with open parallel wire transmission line, including doppler shift. No noise is added to this spectra. The ratio of power in the central peak to the sidebands changes with pitch angle, and the second sideband contains the highest power.

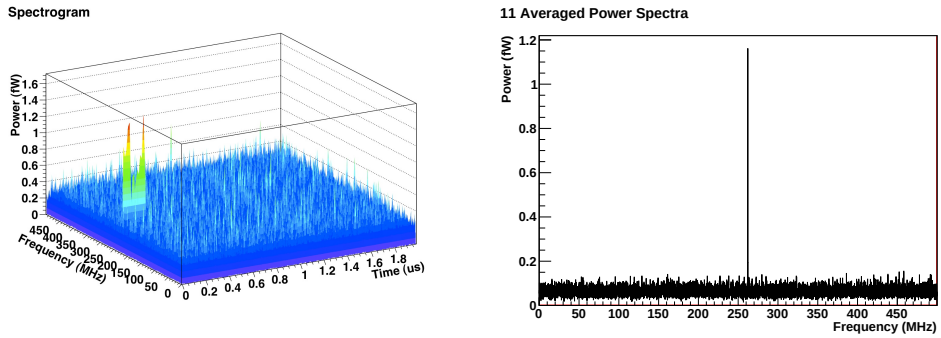

FIG. 9. Spectrograph from a open parallel wire transmission line, including doppler shift and noise. On the right, eleven high-power bins are averaged together but the sidebands are not visible above the noise.

IV. TO DO LIST

- **Realistic Electric Fields:** The grounded trapping coil and dielectric support structure will change the electric fields slightly from the analytic cases. Also, misalignment between wires or strips will affect the fields. These should be included.

- **Misaligned Magnet Coils:** The magnetic fields are calculated assuming axisymmetric coils, but the small trap coil may be off-axis from the large coil. This could affect the frequency of the magnetron drift.

- **Energy Loss near transmission lines:** Currently the simulated electrons loss energy through radiation into free space, but near open transmission lines the rate is about four times higher. For open transmission lines, we limit the observation times to account for the larger energy loss, but do not simulate it.

- **Frequency Dependence of Noise:** Some sources of noise are frequency dependent, but we now assume the noise is white.

- **Power loss due to dielectric:** Losses occur due to resistance in the wires and lossy dielectric. Since the dielectric is low-loss and only occupies a small area around the wires, this has been neglected.

- **Optimal Windowing (Hann Window):** The rectangular window function causes spectral leakage in the Fourier transform. Another window function such as the Hann window may improve the signal to noise for some electron parameters.

- **Matched Filter or Template Filtering:** If the true electron waveform is known, which depends on the magnetic field variation and pitch angle, the optimal signal to noise can be achieved without a Fourier transform, but with a matched filter. Errors in estimating the true waveform compromise the SNR.

---

[1]

[2] 08, 1, p. 0.

[3] Michelle Leber, *Derivation of the power transmitted by various waveguides*, Project8 Internal Note, May 2011. 8, 12

[4] Julius O. Smith, *Spectral audio signal processing, October 2008 draft*, `https://ccrma.stanford.edu/~jos/sasp/sasp.html`, accessed June 2010, online book. 5